Vortex core states in superfluid Fermi-Fermi mixtures with unequal masses

M. Iskin

Joint Quantum Institute, National Institute of Standards and Technology,
and University of Maryland, Gaithersburg, Maryland 20899-8423, USA.
(Dated: August 6, 2008)

We analyze the vortex core states of two-species (mass imbalanced) superfluid fermion mixtures as a function of two-body binding energy in two dimensions. In particular we solve the Bogoliubov-de Gennes equations for a population balanced mixture of ^{6}Li and ^{40}K atoms at zero temperature. We find that the vortex core is mostly occupied by the light-mass (^{6}Li) fermions and that the core density of the heavy-mass (^{40}K) fermions is highly depleted. This is in contrast with the one-species (mass balanced) mixtures with balanced populations where an equal amount of density depletion is found at the vortex core for both pseudospin components.

Recent observation of quantized vortices in two-component mass and population balanced fermion mixtures of ^{6}Li atoms with short-ranged attractive interactions [1] has not only complemented the previously found evidence [2, 3, 4, 5, 6], but also indicated a very strong evidence for the superfluid ground state. In these experiments it has been realized that the ground state evolves smoothly from a Bardeen-Cooper-Schrieffer (BCS) superfluid to a molecular Bose-Einstein condensate (BEC) as the attractive interaction strength varies from small to large values, marking the first demonstration of the the-oretically predicted BCS-BEC crossover [7, 8, 9]. More recently quantized vortices have also been studied in mass balanced but population imbalanced fermion mixtures [10] to investigate more exotic superfluid phases. On the theoretical side vortex core states in superfluid fermion mixtures have been extensively studied for mass and population balanced mixtures [11, 12, 13, 14, 15]. In these works it was predicted that the local density of fermions is slightly depleted at the vortex core for weak interactions, and that the density depletion increases with increasing interaction strength. Furthermore vortex core states of mass balanced but population imbalanced fermion mixtures have recently been analyzed [16, 17], showing that the unpaired (excess) fermions occupy the core states. However these predictions have not been experimentally observed since a probing technique analogous to the scanning tunneling microscopy is still lacking.

Arguably one of the current frontiers of ultracold atom research is the investigation of two-species mass imbalanced fermion mixtures (e.g. ^{6}Li and ^{40}K, ^{6}Li and ^{87}Sr, or ^{40}K and ^{87}Sr) with or without a population imbalance, due to their greater potential for finding exotic phases [18, 19]. Such mixtures are currently of interest to many communities ranging from atomic and molecular to condensed and nuclear matter physics, and recent analysis of the ground state phase diagram have shown quantum and topological phase transitions [20, 21, 22, 23, 24, 25, 26]. In this manuscript, motivated by the very recent experimens on ^{6}Li and ^{40}K mixtures [18, 19], we analyze the vortex core states of

superfluid Fermi-Fermi mixtures with unequal masses as a function of two-body binding energy. In particular we use the Bogoliubov-de Gennes (BdG) formalism to study a population balanced mixture of ^{6}Li and ^{40}K atoms at zero temperature. We find that the vortex core is mostly filled with the light-mass (^{6}Li) fermions and that the core density of the heavy-mass (^{40}K) fermions is highly depleted. This is in contrast with the one-species (mass balanced) mixtures with balanced populations where an equal amount of density depletion is found at the vortex core for both pseudospin components [11, 12, 13, 14, 15].

We achieve these results by using the following Hamiltonian density $H(x) = \sum_\sigma \psi_\sigma^\dagger(x) K_\sigma(\mathbf{r}) \psi_\sigma(x) - g\Psi^\dagger(x)\Psi(x)$, which describes two-component fermion mixtures with attractive ($g > 0$) and short-range interactions. Here $\hbar = k_B = 1$, and $\psi_\sigma^\dagger(x)$ and $\psi_\sigma(x)$ are the Grassmann field operators corresponding to creation and annihilation of pseudospin σ fermions at position $\mathbf{r}$ and time τ ($x \equiv \{\mathbf{r}, \tau\}$). Furthermore $K_\sigma(\mathbf{r}) = -\nabla^2/(2M_\sigma) - \mu_\sigma$ and $\Psi(x) = \psi_\downarrow(x)\psi_\uparrow(x)$, where M_σ is the mass and μ_σ is the chemical potential of σ fermions. In the mean-field approximation for the superfluid phase the resultant Hamiltonian can be diagonalized via the Bogoliubov-Valatin transformation $\psi_\sigma(\mathbf{r}) = \sum_n [u_{n,\sigma}(\mathbf{r})\gamma_{n,\sigma} - s_\sigma v_{n,\sigma}^*(\mathbf{r})\gamma_{n,-\sigma}^\dagger]$, where $u_{n,\sigma}(\mathbf{r})$ and $v_{n,\sigma}(\mathbf{r})$ are the amplitudes and $\gamma_{n,\sigma}^\dagger$ and $\gamma_{n,\sigma}$ are the operators corresponding to the creation and the annihilation of pseudospin σ quasiparticles, and $s_\uparrow = +1$ and $s_\downarrow = -1$. Then the single particle Green's function matrix (in Nambu pseudospin space) can be written as

$$\mathbf{G}(\mathbf{r}, \mathbf{r}'; i\omega_\ell) = \sum_{n,\sigma} \frac{\varphi_{\mathbf{n},\sigma}(\mathbf{r})\varphi_{\mathbf{n},\sigma}^\dagger(\mathbf{r}')}{i\omega_\ell - s_\sigma \epsilon_{n,\sigma}}, \quad (1)$$

where $\omega_\ell = (2\ell + 1)\pi T$ is the fermionic Matsubara frequency, ℓ is an integer number and T is the temperature. Here $\varphi_{\mathbf{n},\sigma}(\mathbf{r})$ and $\epsilon_{n,\sigma} > 0$ are the eigenfunctions and the eigenvalues of the BdG equations

$$\begin{bmatrix} K_\uparrow(\mathbf{r}) & \Delta(\mathbf{r}) \\ \Delta^*(\mathbf{r}) & -K_\downarrow^*(\mathbf{r}) \end{bmatrix} \varphi_{\mathbf{n},\sigma}(\mathbf{r}) = s_\sigma \epsilon_{n,\sigma} \varphi_{\mathbf{n},\sigma}(\mathbf{r}), \quad (2)$$

where $\varphi_{\mathbf{n},\sigma}(\mathbf{r})$ is given by $\varphi_{\mathbf{n},\uparrow}^\dagger(\mathbf{r}) = [u_{n,\uparrow}^*(\mathbf{r}), v_{n,\downarrow}^*(\mathbf{r})]$ for

the $\uparrow$ and $\varphi_{\mathbf{n},\downarrow}^\dagger(\mathbf{r}) = [v_{n,\uparrow}(\mathbf{r}), -u_{n,\downarrow}(\mathbf{r})]$ for the $\downarrow$ eigenvalues. Since the BdG equations are invariant under the transformation $v_{n,\uparrow}(\mathbf{r}) \to u_{n,\uparrow}^*(\mathbf{r})$, $u_{n,\downarrow}(\mathbf{r}) \to -v_{n,\downarrow}^*(\mathbf{r})$ and $\epsilon_{n,\downarrow} \to -\epsilon_{n,\uparrow}$, it is sufficient to solve only for $u_n(\mathbf{r}) \equiv u_{n,\uparrow}(\mathbf{r})$, $v_n(\mathbf{r}) \equiv v_{n,\downarrow}(\mathbf{r})$ and $\epsilon_n \equiv \epsilon_{n,\uparrow}$ as long as we keep all of the solutions with positive and negative eigenvalues.

In Eq. (2) $\Delta(\mathbf{r})$ is the local superfluid order parameter defined by $\Delta(\mathbf{r}) = g\langle\psi_\uparrow(\mathbf{r})\psi_\downarrow(\mathbf{r})\rangle = -gT\sum_\ell G_{\uparrow,\downarrow}(\mathbf{r},\mathbf{r};i\omega_\ell)$, which after evaluating the frequency sum leads to $\Delta(\mathbf{r}) = -g\sum_{n,\sigma} s_\sigma u_{n,\sigma}(\mathbf{r})v_{n,-\sigma}^*(\mathbf{r})f(s_\sigma\epsilon_{n,\sigma})$. Here $\langle...\rangle$ is a thermal average and $f(x) = 1/[\exp(x/T) + 1]$ is the Fermi function. Using the symmetry of the BdG equations this equation can be written as $\Delta(\mathbf{r}) = -g\sum_n u_n(\mathbf{r})v_n^*(\mathbf{r})f(\epsilon_n)$. We also relate the interaction strength g to the two-body binding energy $\epsilon_b < 0$ of an $\uparrow$ and a $\downarrow$ fermion via the relation $1/g = (1/A)\sum_\mathbf{k} 1/(\epsilon_{\mathbf{k},\uparrow} + \epsilon_{\mathbf{k},\downarrow} - \epsilon_b)$, where A is the area of the sample and $\epsilon_{\mathbf{k},\sigma} = k^2/(2M_\sigma)$ is the kinetic energy. This leads to $g = 4\pi/[M_r \ln(1 - 2\epsilon_c/\epsilon_b)]$, where $M_r = 2M_\uparrow M_\downarrow/(M_\uparrow + M_\downarrow)$ is twice the reduced mass of an $\uparrow$ and a $\downarrow$ fermion and ϵ_c is the energy cutoff used in the $\mathbf{k}$-space integration. The order parameter equation has to be solved self-consistently with the number equations $N_\sigma = \int d\mathbf{r} n_\sigma(\mathbf{r})$ to determine μ_σ, where $n_\sigma(\mathbf{r}) = \langle\psi_\sigma^\dagger(\mathbf{r})\psi_\sigma(\mathbf{r})\rangle = s_\sigma \lim_{\tau\to 0^+} T\sum_\ell e^{is_\sigma\omega_\ell\tau}G_{\sigma,\sigma}(\mathbf{r},\mathbf{r};i\omega_\ell)$ is the local density of σ fermions. After evaluating the frequency sum this relation leads to $n_\sigma(\mathbf{r}) = \sum_n[|u_{n,\sigma}(\mathbf{r})|^2 f(\epsilon_{n,\sigma}) + |v_{n,\sigma}(\mathbf{r})|^2 f(-\epsilon_{n,-\sigma})]$, which can be written as $n_\uparrow(\mathbf{r}) = \sum_n |u_n(\mathbf{r})|^2 f(\epsilon_n)$ and $n_\downarrow(\mathbf{r}) = \sum_n |v_n(\mathbf{r})|^2 f(-\epsilon_n)$ by using the symmetry of the BdG equations. Having discussed the BdG formalism, next we analyze the self-consistency equations for a single vortex.

In particular we consider a two-dimensional homogenous disk of radius R such that the local order parameter can be written as $\Delta(\mathbf{r}) = \Delta(r)\exp(-i\kappa\theta)$, where $\mathbf{r} = (r,\theta)$ are the polar coordinates and κ is the vortex winding number. This choice is due to numerical reasons and we do not expect any qualitative difference between our results and the three-dimensional ones. Then the normalized wave functions are of the form $u_n(\mathbf{r}) = u_{n,m}(r)\exp(im\theta)/\sqrt{2\pi}$ and $v_n(\mathbf{r}) = v_{n,m}(r)\exp[i(m+\kappa)\theta]/\sqrt{2\pi}$ such that the BdG equations can be solved separately in each subspace of fixed angular momentum m [11]. We further project the radial wave functions $u_{n,m}(r) = \sum_j c_{n,j}\phi_{j,m}(r)$ and $v_{n,m}(r) = \sum_j d_{n,j}\phi_{j,m+\kappa}(r)$ onto a set of orthonormal Bessel functions $\phi_{j,m}(r) = \sqrt{2}J_m(\alpha_{j,m}r/R)/[RJ_{m+1}(\alpha_{j,m})]$, where the argument $\alpha_{j,m}$ is the jth zero of $J_m(x)$. This procedure reduces BdG equations given in Eq. (2) to a $2j_{max} \times 2j_{max}$ matrix eigenvalue problem [11]

$$\sum_{j,j'}\begin{pmatrix} K_{\uparrow,m}^{j,j'} & \Delta_m^{j,j'} \\ \Delta_m^{j',j} & -K_{\downarrow,m+\kappa}^{j',j} \end{pmatrix}\begin{pmatrix} c_{n,j'} \\ d_{n,j'} \end{pmatrix} = \epsilon_n \sum_j \begin{pmatrix} c_{n,j} \\ d_{n,j} \end{pmatrix}, (3)$$

if we allow $1 \le j \le j_{max}$ states. Here $K_{\sigma,m}^{j,j'} =$ $[\alpha_{j,m}^2/(2M_\sigma R^2) - \mu_\sigma]\delta_{j,j'}$ is the diagonal and $\Delta_m^{j,j'} = \int rdr\Delta(r)\phi_{j,m}(r)\phi_{j',m+\kappa}(r)$ is the off-diagonal element where $\delta_{i,j}$ is the Kronecker delta. Furthermore the order parameter equation reduces to

$$\Delta(r) = -g\sum_{n,m,j,j'}\frac{c_{n,j}d_{n,j'}}{2\pi}\phi_{j,m}(r)\phi_{j',\widetilde{m}}(r)f(\epsilon_n), \quad (4)$$

and the local density equations reduce to

$$n_\uparrow(r) = \sum_{n,m,j,j'}\frac{c_{n,j}c_{n,j'}}{2\pi}\phi_{j,m}(r)\phi_{j',m}(r)f(\epsilon_n), \quad (5)$$

$$n_\downarrow(r) = \sum_{n,m,j,j'}\frac{d_{n,j}d_{n,j'}}{2\pi}\phi_{j,\widetilde{m}}(r)\phi_{j',\widetilde{m}}(r)f(-\epsilon_n), (6)$$

where $\widetilde{m} = m + \kappa$. Notice that the total numbers of $\uparrow$ and $\downarrow$ fermions are given by $N_\uparrow = \sum_{n,m,j} c_{n,j}^2 f(\epsilon_n)$ and $N_\downarrow = \sum_{n,m,j} d_{n,j}^2 f(-\epsilon_n)$, respectively. We emphasize that these mean-field equations can be used for all values of g but they only provide a qualitative description of BCS-BEC crossover at zero temperature ($T = 0$) as discussed next.
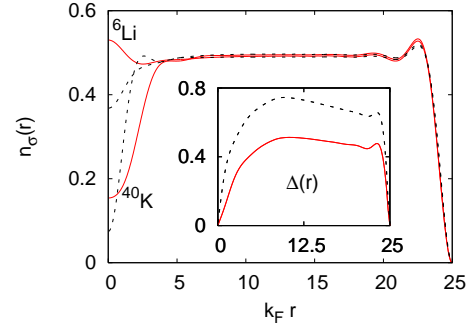

FIG. 1: (Color online) Local density of σ fermions $n_\sigma(r)$ [in units of $k_F^2/(2\pi)$] versus radius r (in units of $1/k_F$) is shown for a population balanced mixture of ^{6}Li and ^{40}K atoms. Here $|\epsilon_b| = 0.1\epsilon_F$ (solid lines) and $|\epsilon_b| = 0.2\epsilon_F$ (dotted lines). The inset shows the local order parameter $\Delta(r)$ (in units of ϵ_F) versus r for the same parameters.

In this manuscript we discuss a population balanced mixture of ^{6}Li and ^{40}K atoms, where $N_\uparrow = N_\downarrow$ and $M_\uparrow = 0.15M_\downarrow$. For this purpose we set a large energy cutoff $\epsilon_c = 9\epsilon_F$, and numerically solve the self-consistency Eqs. (3), (4), (5), and (6) for a singly quantized vortex with $\kappa = 1$ at $T = 0$. Here $\epsilon_F = k_F^2/(2M_r)$ is a characteristic energy scale where k_F is the Fermi momentum corresponding to the total density of fermions. We also choose $R = 25/k_F$ as the radius of the two-dimensional disc, and $j_{max} = 25$ and $|m|_{max} = 50$ as the maximum quantum numbers. Notice that the bulk density $n_\sigma = N_\sigma/A$ is given by $n_\uparrow = n_\downarrow = k_F^2/(4\pi)$ for a population balanced mixture. As one may expect presence of a single vortex can not significantly effect the bulk parameters. Therefore, to simplify the numerical calculations, we first solve μ_σ and $|\Delta_0|$ self-consistently for a

vortex-free system, and then use these solutions as an input for our vortex calculation. Here $|\Delta_0|$ corresponds to the bulk value of $\Delta(r)$. Since our vortex calculation is not fully self-consistent, $N_\uparrow$ and $N_\downarrow$ turn out to be very close $|N_\uparrow - N_\downarrow| \sim 10^{-3}(N_\uparrow + N_\downarrow)$ but not exactly the same. Furthermore, for mass balanced mixtures, we checked that this procedure gives results that are in qualitative agreement with the earlier works on population balanced [11, 12, 13, 14, 15] as well as population imbalanced systems [16, 17].

In Fig. 1 we show $n_\sigma(r)$ for a population balanced mixture of ^{6}Li and ^{40}K atoms. We also show $\Delta(r)$ as an inset for the same parameters. When g is small such that $|\epsilon_b| \ll \epsilon_F$, the vortex core is mostly filled with the light-mass (^{6}Li) fermions while core density of the heavy-mass (^{40}K) fermions is highly depleted. This is because the bound state energy spectrum is discrete with a small but nonzero separation $\sim |\Delta_0|^2/\epsilon_F$ (discussed below), and thus only the light-mass fermions can occupy these states at the core since $\mu_{Li} > \mu_K$ due to the mass difference. While this is in sharp contrast with mass and population balanced mixtures where the bound states are unoccupied and equal amount of depletion occurs for both σ fermions [11, 12, 13, 14, 15], it is similar to mass balanced but population imbalanced mixtures where the core is filled with excess fermions due to their higher chemical potential [16, 17]. However, as shown in Fig. 1, local density of the light-mass fermions as well as that of the heavy-mass one deplete more with increasing $|\epsilon_b|$, which is qualitatively similar to that of mass balanced mixtures where the local density depletion also increases with increasing g [13, 14, 15]. This is because the energy separation between the bound states increases with increasing $|\Delta_0|$ which makes them less occupied. To further understand these peculiar density depletions, next we analyze the single particle density of states for σ fermions as well as the spectrum of energy eigenvalues.

At $T = 0$ the local single particle density of states for σ fermions is defined by $D_\sigma(\mathbf{r}, \omega) = -(1/\pi)\mathrm{Im}[\lim_{\varepsilon\to 0^+} G_{\sigma,\sigma}(\mathbf{r}, \mathbf{r}; i\omega_\ell \to \omega + i\varepsilon)]$. This leads to $D_\sigma(\mathbf{r}, \omega) = \sum_n[|u_{n,\sigma}(\mathbf{r})|^2\delta(\omega - \epsilon_{n,\sigma}) + |v_{n,\sigma}(\mathbf{r})|^2\delta(\omega + \epsilon_{n,-\sigma})]$ where $\delta(x)$ is the delta function, and it can be written as $D_\uparrow(\mathbf{r}, \omega) = \sum_n |u_n(\mathbf{r})|^2\delta(\omega - \epsilon_n)$ and $D_\downarrow(\mathbf{r}, \omega) = \sum_n |v_n(\mathbf{r})|^2\delta(\omega + \epsilon_n)$ by using the symmetry of the BdG equations. Then the overall single particle density of states is found by $D_\sigma(\omega) = \int d\mathbf{r} D_\sigma(\mathbf{r}, \omega)$, which for a single vortex reduces to $D_\uparrow(\omega) = \sum_{n,m,j} c_{n,j}^2\delta(\omega - \epsilon_n)$ and $D_\downarrow(\omega) = \sum_{n,m,j} d_{n,j}^2\delta(\omega + \epsilon_n)$. We use a small spectral broadening ($0.01\epsilon_F$) to regularize these delta functions.

In Fig. 2 we show $D_\sigma(\omega)$ for a population balanced mixture of ^{6}Li and ^{40}K atoms. We also show the spectrum of energy eigenvalues ϵ_n as an inset for the same parameters. Similar to mass balanced mixtures [11, 12, 13, 14, 15], the positive and negative energy spectra are connected by a single branch of discrete Andreev-like bound states. The visible discreteness of the continuum spectrum shown in Fig. 2 is a finize size ef-
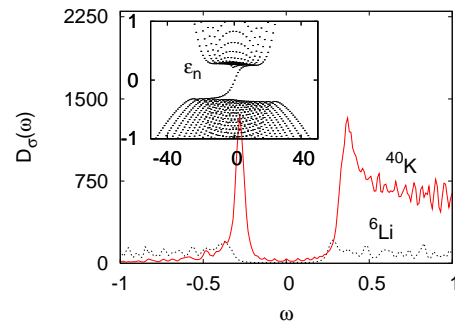

FIG. 2: (Color online) Single particle density of states for σ fermions $D_\sigma(\omega)$ (in units of $1/\epsilon_F$) versus energy ω (in units of ϵ_F) is shown for a population balanced mixture of ^{6}Li and ^{40}K atoms. Here $|\epsilon_b| = 0.1\epsilon_F$. The inset shows the spectrum of energy eigenvalues ϵ_n (in units of ϵ_F) versus angular momentum m for the same parameters.

fect and the spectrum becomes continuous only in the thermodynamic limit ($k_F R \to \infty$), while the discreteness of the bound states is insensitive to the system size since these states are strongly localized around the vortex core. However the energy spectrum is asymmetric around $\epsilon_n = 0$ with less bound and continuum states for $\epsilon_n > 0$, which is due to the broken pseudospin symmetry since the masses ($m_K > m_{Li}$) and therefore the chemical potentials ($\mu_{Li} > \mu_K$) are different for $\uparrow$ and $\downarrow$ fermions. This is in sharp contrast with mass and population balanced mixtures where the energy spectrum is symmetric [14, 15].

Furthermore the energy spectrum is qualitatively different on the positive and the negative ω sides, and it is very illustrative to make an analogy between the energy spectrum of mass imbalanced mixtures shown in Fig. 2 and that of the mass balanced mixtures [14, 15]. For mass and population balanced mixtures energy spectra that are qualitatively similar to the negative (positive) side with many (few) bound and continuum states occur for small (large) values of $|\epsilon_b|$, leading to low (high) density depletions at the vortex core. This analogy suggests that the local vortex core density of the heavy-mass fermions should deplete more than that of the light-mass fermions since the density of states for heavy-mass fermions is higher (lower) for positive (negative) ω. We also find that the bound state contribution to $n_\sigma(r)$ is a nonmonotonic function of r with a maximum at an intermediate distance $r = r_*$. This nonmonotonic contribution is due to the strongly localized quasiparticle amplitudes that are associated with the bound states, which also give rise to Friedel-like $\Delta(r)$ oscillations around the vortex core in the strict BCS limit [11, 12, 13, 14]. Therefore the unequal density depletions shown in Fig. 1 are purely density of states effects arising from the asymmetric energy spectrum shown in Fig. 2. Next we analyze the density as well as the velocity of the superfluid fermions.

The quantum mechanical probability current operator for σ fermions is given by

$\widehat{\mathbf{J}}_\sigma(\mathbf{r}) = [1/(2M_\sigma i)][\psi_\sigma^\dagger(\mathbf{r})\nabla\psi_\sigma(\mathbf{r}) - H.c.]$ where $H.c.$ is the Hermitian conjugate. Therefore the local current density $\mathbf{J}_\sigma(\mathbf{r}) = \langle\widehat{\mathbf{J}}_\sigma(\mathbf{r})\rangle$ circulating around a single vortex becomes $\mathbf{J}_\uparrow(\mathbf{r}) = [1/(2M_\uparrow i)]\sum_n[u_n^*(\mathbf{r})\nabla u_n(\mathbf{r})f(\epsilon_n) - H.c.]$ for the $\uparrow$ and $\mathbf{J}_\downarrow(\mathbf{r}) = [1/(2M_\downarrow i)]\sum_n[v_n(\mathbf{r})\nabla v_n^*(\mathbf{r})f(-\epsilon_n) - H.c.]$ for the $\downarrow$ fermions where we used the symmetry of the BdG equations. These relations can be written as $\mathbf{J}_\sigma(\mathbf{r}) = n_0(\mathbf{r})\mathbf{v}_\sigma(\mathbf{r})/2$, where $n_0(\mathbf{r})$ is the local superfluid density and $\mathbf{v}_\sigma(\mathbf{r}) = \kappa\widehat{\theta}/(2M_\sigma r)$ is the local superfluid velocity. Therefore $\mathbf{J}_\sigma(\mathbf{r})$ is along the $\widehat{\theta}$ direction, and for a single vortex it is given by $J_\uparrow(r) = [1/(2\pi M_\uparrow r)]\sum_{n,m} m[\sum_j c_{n,j}\phi_{j,m}(r)]^2 f(\epsilon_n)$ for the $\uparrow$ and $J_\downarrow(r) = -[1/(2\pi M_\downarrow r)]\sum_{n,m}(m + \kappa)[\sum_j d_{n,j}\phi_{j,m+\kappa}(r)]^2 f(-\epsilon_n)$ for the $\downarrow$ fermions such that $n_0(r) = (4M_\sigma/\kappa)rJ_\sigma(r)$.
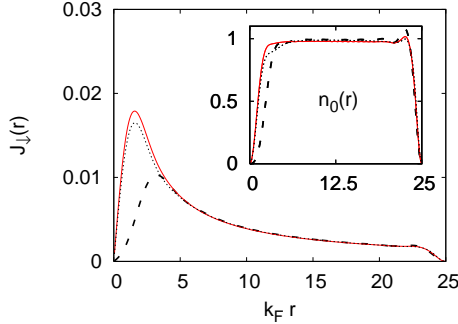

FIG. 3: (Color online) Local current density $J_\downarrow(r)$ [in units of $M_\downarrow/k_F^3$] versus radius r (in units of $1/k_F$) is shown for a population balanced mixture of ^{6}Li and ^{40}K atoms. Here $|\epsilon_b| = 0.1\epsilon_F$ (dashed line), $|\epsilon_b| = 0.3\epsilon_F$ (solid line) and $|\epsilon_b| = 0.5\epsilon_F$ (dotted line). The inset shows the local superfluid fermion density $n_0(r)$ [in units of $k_F^2/(2\pi)$] versus r for the same parameters.

In Fig. 3 we show $J_\downarrow(r)$ for a population balanced mixture of ^{6}Li and ^{40}K atoms. We also show $n_0(r)$ as an inset for the same parameters. The bound states have positive (paramagnetic) and the continuum states have negative (diamagnetic) contribution to $J_\downarrow(r)$. This leads to a nonmonotonic $J_\downarrow(r)$ which first increases as $\propto r$ and then decreases as $\propto 1/r$. The latter behavior is due to the saturation of $n_0(r)$ for long distances away from the vortex core. Therefore a maximum peak current occurs for all values of $|\epsilon_b|$ at some distance r_c away from the vortex core. However the value of this peak current increases until $|\epsilon_b| \simeq 0.3\epsilon_F$ and then decreases for higher values of $|\epsilon_b|$. Since a two-body bound state exists even for an arbitrarily small $g > 0^+$ in two dimensions, we emphasize that this nonmonotonic evolution is not due to the occurrence of a two-body bound state threshold (divergence of the two-body scattering length), as previously suggested for mass and population balanced mixtures in three dimensions [15]. We believe that it is related to the nonmonotonic evolution of the coherence length ξ_c which can be easily extracted from $n_0(r)$. This is qualitatively consistent with the recent experiments involving mass and population balanced mixture of ^{6}Li atoms, where a pronounced peak of critical velocity has been observed on the molecular side of the strongly interacting regime in one-dimensional optical lattices [27].

In summary we analyzed the vortex core states of population balanced ^{6}Li and ^{40}K mixture at $T = 0$ as a function of two-body binding energy. We found that the vortex core is mostly occupied by the light-mass (^{6}Li) fermions and that the core density of the heavy-mass (^{40}K) fermions is highly depleted. This is in contrast with mass and population balanced mixtures where an equal amount of density depletion is found at the vortex core for both pseudospin components.

[1] M. W. Zwierlein *et al.*, Nature (London) **435**, 1047 (2005).

[2] C. A. Regal, M. Greiner, and D. S. Jin, Phys. Rev. Lett. **92**, 040403 (2004).

[3] J. Kinast *et al.*, Phys. Rev. Lett. **92**, 150402 (2004).

[4] M. Bartenstein *et al.*, Phys. Rev. Lett. **92**, 203201 (2004).

[5] T. Bourdel *et al.*, Phys. Rev. Lett. **93**, 050401 (2004).

[6] G. B. Partridge *et al.*, Phys. Rev. Lett. **95**, 020404 (2005).

[7] A. J. Leggett, J. Phys. (Paris) **C7**, 19 (1980).

[8] P. Noziéres and S. Schmitt-Rink, J. Low. Temp. Phys. **59**, 195 (1985).

[9] C. A. R. Sá de Melo, M. Randeria, and J. R. Engelbrecht, Phys. Rev. Lett. **71**, 3202 (1993).

[10] M. W. Zwierlein *et al.*, Science **311**, 492 (2006).

[11] F. Gygi and M. Schlüter, Phys. Rev. B **43**, 7609 (1991).

[12] N. Nygaard *et al.*, Phys. Rev. Lett. **90**, 210402 (2003); Phys. Rev. A **69**, 053622 (2004).

[13] A. Bulgac and Y. Yu, Phys. Rev. Lett. **91**, 190404 (2003).

[14] M. Machida and T. Koyama, Phys. Rev. Lett. **94**, 140401 (2005).

[15] R. Sensarma, M. Randeria, and Tin-Lun Ho, Phys. Rev. Lett. **96**, 090403 (2006).

[16] M. Takahashi *et al.*, Phys. Rev. Lett. **97**, 180407 (2006).

[17] Hui Hu, Xia-Ji Liu, and P. D. Drummond, Phys. Rev. Lett. **98**, 060406 (2007).

[18] M. Taglieber *et al.*, Phys. Rev. Lett. **100**, 010401 (2008).

[19] E. Wille *et al.*, Phys. Rev. Lett. **100**, 053201 (2008).

[20] M. Iskin and C. A. R. Sá de Melo, Phys. Rev. Lett. **97**, 100404 (2006); Phys. Rev. A **76**, 013601 (2007); Phys. Rev. A 77, 013625 (2008).

[21] Shin-Tza Wu, C.-H. Pao, and S.-K. Yip, Phys. Rev. B **74**, 224504 (2006); Phys. Rev. A **76**, 053621 (2007).

[22] G.-D. Lin, W. Yi, and L.-M. Duan, Phys. Rev. A **74**, 031604(R) (2006).

[23] M. M. Parish *et al.*, Phys. Rev. Lett. **98**, 160402 (2007).

[24] J. von Stecher, C. H. Greene, and D. Blume, Phys. Rev. A **76**, 053613 (2007).

[25] M. Iskin and C. J. Williams, Phys. Rev. A **77**, 013605 (2008).

[26] G. Orso, L. P. Pitaevskii, and S. Stringari, Phys. Rev. A **77**, 033611 (2008).

[27] D. E. Miller *et al.*, Phys. Rev. Lett. **99**, 070402 (2007).